

**POTENTIAL APPLICATION OF WIRE WOVEN MESH AS TOWER  
PACKING SUPPORT-COMPUTATIONAL APPROACH**V. Ebrahimejad<sup>1</sup>, A. Sharifian<sup>2</sup><sup>1-2</sup> Department of Mechanical and Electrical Engineering, University of Southern Queensland,  
Toowoomba, Australia

Email: Vahid.ebrahimejad@usq.edu.au

**Keywords:** Wire woven screens, Tower packing support, Wire bulk cross (WBC), Finite element analysis (FEA), Computational fluid dynamics (CFD)**ABSTRACT**

Wire woven metals are new type of truss-like periodic cellular metals (PCM) that have several applications ranging from different loading applications to filtering processes. Their lightness, decent structural integrity and other thermo-fluid mechanics have resulted in a multi-functional structure. Wire bulk cross (WBC), that represents the 3D model of wire woven screens, recently recognised as the premier truss-like PCM in terms of normalized compressive and shear strength. In addition, it shows decent resistance to buckling effects. Homogeneity of these structures can also provide a uniform flow with minimal pressure drop and velocity perturbation in industries that maintaining design and operating conditions of flow is critical. In Oil & Gas industry, packing towers imply an essential requirement that operating conditions of vapor flows should remain unchanged, while heavy random packings, mounted on the top, are well-supported. Thus, investigation on effects of wire woven mesh screen aperture size on its structural integrity, while minimising flow pressure-drop and velocity profile changes can introduce these truss-like structures as tower packing supports. In this research, using FEA, wire woven mesh screens undergo several aperture sizes to investigate the mechanical behaviour of the structure. Similarly, CFD analysis conducted to simulate the behaviour of vapor flows through these wire woven mesh screens. The numerical results are then plotted against both porosity ratio and aperture size to indicate the mechanical and flow behaviour patterns. In the CFD analysis graphs, flooding point of the nominated nitrogen flow is shown to give an inside into the points when flow might enter flooded region. Results showed deflection of the mesh under the load, fluid velocity profile and pressure drop values level off after certain sizes are reached. Normalized combination of these analysis can then be used to optimise and determine acceptable aperture size ranges that meet the requirements in specific industry applications.

**1 INTRODUCTION**

Wire woven mesh metals, particularly WBC, are given more credit in several applications as sandwich panels, heavy loadings, shock absorptions, and as a medium for paper making filtering process. The homogeneity, uniformly laid-out structure, and high void fraction in 3D structures, such as WBC, give them a unique applicability in fluid flow processes. WBC can also be used in load supporting applications when compression and shear stresses are remarkable.

Research on unique characteristics of wire woven mesh metals is at its early stage. However, Kang et al. found the high compatibility of WBC, that represents the 2D wire woven mesh screens, when compared to metal foams. In terms of mechanical behaviours, Zitha *et al.* findings indicated that normalized compressive strength and moduli of semi-WBC (consists of multiple parallel layers of straight wire mesh screens that are connected to each other by helically formed wires) and straight WBC are relatively higher than their competitors WBD, WBK and common helically-woven WBC [2]. This finding shows using straight wires, compared to formed ones can reduce the manufacturing costs when the mechanical characteristics of the structure remains at higher level. In terms of the effects of aperture size on total structural integrity, Lee *et al.* indicates that when WBC aperture size increases, the buckling tendency of the structure remains unchanged; this unique mechanical behavior did not apply to the rest

of truss like PCMs. It is also pointed out that for relative density of 1%-5%, WBC can act as an optimized and effective structure against both compression and shear loads [3]. Thus, this extraordinary behavioral pattern for straight WBC, ensures that by achieving higher voids (aperture sizes) within the structure, pressure drop and velocity perturbation of any flow through this medium can also be minimized.

In terms of fluid dynamics, research has been conducted using computational fluid analysis of fluids passing through a 2D representative of wire woven bulk cross, WBC. Sheldon *et al.* investigations focused on subtle distance alternation between filaments and their influence on the flow rate. It is concluded that if the normalized distances between filament,  $L$ , increase by an amount of  $\varepsilon = \frac{\Delta L}{L}$ , provided that  $|\varepsilon| < 0.3$ , the rate of flow can increase by  $2\varepsilon$ . This indicates aperture size enlargement can bring about a considerable flow rate increase. However, perturbed and non-homogenous fabric geometry of the structure will result in a major velocity fall in the neighboring wires [4]. Therefore, during this research, aperture size among the wires maintained homogenous.

In industry, absorption and distillation processes are carried out using trayed or packed towers. Packing towers are preferable, due to lower maintenance, accessibility and replacement activities. In Oil & Gas industry, packing arrangement is mostly structured (eg. stacked rings, grids) or random (eg. rings, saddles). The voids between packings act as a medium that provides a suitable platform for liquid-gas interactions process. Packing elements' materials range from ceramics, plastics to metals that need to be well-supported by suitable packing supports.

To maintain high efficiency and performance, vapors should experience least amount of pressure drop while maintaining uniform velocity profile before entering the packing voids. This implies that demisters and packing supports minimize the disturbance for vapor flows, resulting in a condition where vapor flows upward through the packing section while liquid moves downward when pre-defined operating conditions remain unchanged [5]. To meet these objectives, the packing supports should have a decent structural integrity, homogeneity and maximum aperture size. Consideration of wire woven metals, particularly WBC, as an alternative solution for this purpose can help in reducing vapor pressure drops, perturbed velocity profiles, final cost, in addition to maintaining operating conditions and structural integrity of packing support. Coulson and Richardson also propose that maximized vapor design velocity is normally between 80-85% of flooding velocity [6]. Thus, optimized wire woven meshes can also prevent vapor flooding within the packing, that normally occurs when operating velocity exceeds 25% of its designed value.

This research aims to study the potential application of straight and semi-straight WBC as tower packing supports. This objective is evaluated through modelling 2D straight wire mesh screens undergoing variable aperture sizes. This is followed by conducting computational analysis using finite element analysis and computational fluid dynamics to have a decent clarification on effect of aperture size on solid mechanics and fluid dynamics characteristics of the metal mesh screen and the vapor flow, respectively. Validations are considered by comparing the numerical results with mathematical models proposed by other authors. Results are discussed in section 3, and conclusion is explained in section 4.

## 2 METHODS

### 2.1 Materials

The STEEL SUS-304 with the mechanical properties mentioned in the Table 1 is used for the FEA analysis. As this material has been used by other researchers for evaluation of mechanical properties of different types of truss-like wire woven mesh metals, it will provide a platform for better comparisons. Based on the current Oil & Gas tower design principles, aperture sizes are selected based on maximum size of commonly used C-Ring random packing, which is 75 mm, for larger packing towers to 20 mm, for smaller diameter towers. Thus, meshes are laid out to form a 70×70 mm to 20×20 mm size by 5 mm increments to ensure accurate results. Table 2 shows how random packings sizes are selected based on tower diameter.

Material	Young's modulus (GPa)	Density (kg/m <sup>3</sup> )	Tensile Yield Strength (MPa)	Poisson Ratio
STEEL SUS 304	200	7850	250	0.30

Table 1: Mechanical properties of Stainless-steel SUS 304

Column Diameter (m)	Use Packing Size (mm (in))
< 0.3 m (1 ft)	25 mm (1 in.)
0.3 to 0.9 m (1 to 3 ft)	25 to 38 mm (1 to 1.5 in.)
> 0.9 m	50 to 75 mm (2 to 3 in.)

Table 2: Random packing size selection according to tower diameters [7].

## 2.2 Computational inputs

Finite element analysis for all the cases conducted using SolidWorks for geometrical modelling and Ansys Workbench (Mechanical) for stress analysis. After selection of stainless steel, SUS 304, with 20-70 mm aperture sizes, wire diameter fixed uniformly as 7 mm for both FEA and CFD analysis. To evaluate the worst-case scenario the heaviest C-Ring random packing with 207 kg/m<sup>3</sup> and 97% void fraction selected from Sulzer Chemtech Ltd. This maximum practical load is then uniformly distributed around the mesh screen nodal points to ensure loads caused by random packings are well-simulated. Metal mesh screens are then fixed to represent the welding supports in tower internal walls. Figure 1, part A, indicates the simulated screen meshes with a variable aperture size (70:5:20).

Computational fluid dynamics for the models is done by Ansys Workbench (Fluent). Nitrogen ( $N_2$ ) is present in several chemical processes in petrochemical plants. It is used both for absorption (eg. stripping) and distillation processes, when impurities of gas mixture are removed or separated. Nitrogen is then selected as the medium for computational fluid analysis. Based on typical steady state absorption processes,  $N_2$  vapor had 1.06 m/s when flowed through the wire woven mesh screen. Reynold number,  $Re_s$ , that is for screen, approximately ranged from 400-700 while  $Re_a$ , that is based on wire diameter and freestream velocity was almost 400. All the measurements, including pressure drops and flow velocity before and after the metal mesh screens have been through the center point of middle apertures. The outlet velocities are measured at fixed distances (100 mm) from metal mesh screen, to represent the vapor entering the packing voids. In part B and C in Figure 1, considerable upstream flow (500 mm) and mesh refinements around metal screens are shown, respectively.

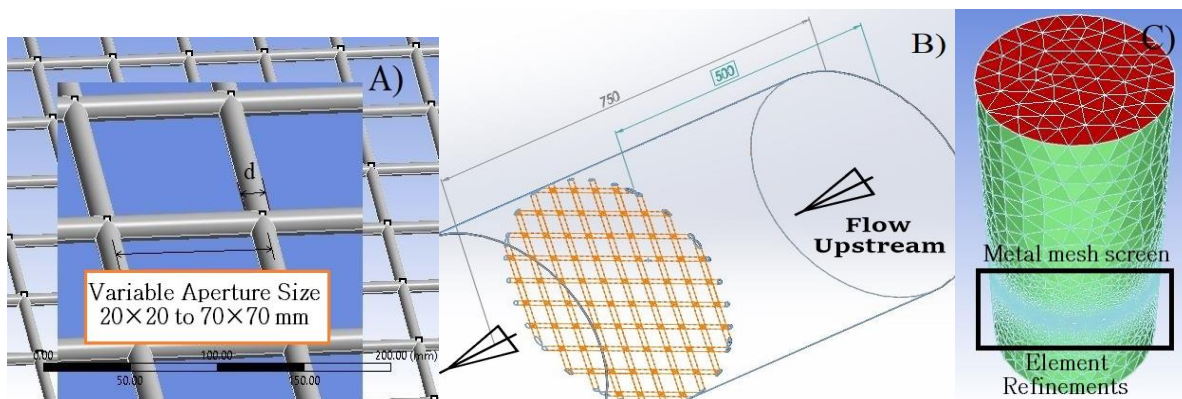


Figure 1: A) Variable metal mesh screen. B) upstream vapor flow simulation C) Mesh refinement.

**3 RESULTS AND DISCUSSIONS**

**3.1 CFD & FEA plots for variable aperture sizes**

The FEA analysis for ten cases of metal screen mesh reveals that as the aperture size increases, the maximum displacement within the whole structure grows exponentially. This maximum deflection that occurs in the central part of the woven mesh metal, tend to level off when it reaches a certain  $\frac{d}{L}$  ratio. As previously mentioned, in this research, the  $\frac{d}{L}$  ratio is based on the constant size increments of 5mm for each of ten cases. However, in both FEA cases the variables are decreasing, the tendency for leveling off is less sensible for nominated case of Von mises stresses (Figure 2).

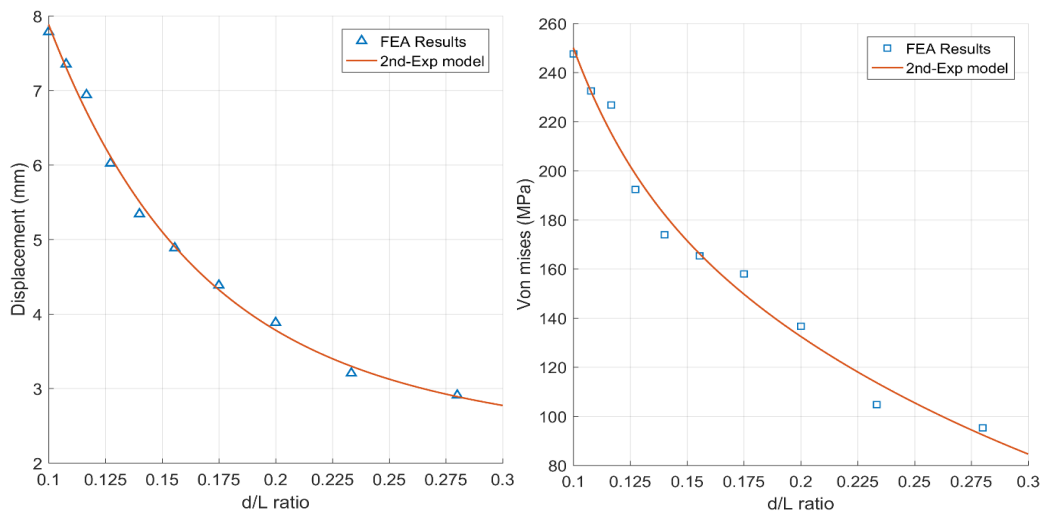


Figure 2: Maximum displacement and Von mises stresses for ten aperture sizes.

Figure 3 shows a sample CFD result when  $\frac{d}{L} = 0.1$ , and the aperture size is 70×70 mm. As throughout the CFD analysis, the measurements are along centerlines (Part B), the importance of streamlines at both sides of metal wires are neglected. However, these red lines represent a sudden rise in local velocities that can affect the flooding conditions in the voids, where liquid-gas interactions occur (Part A). Small development of vortices is also detected which can open-up a new field of research to optimize the metal wire diameters to decrease the number of eddies and vortices. Part B, also indicates the stagnation points with red colors where the total pressure reach maximum values.

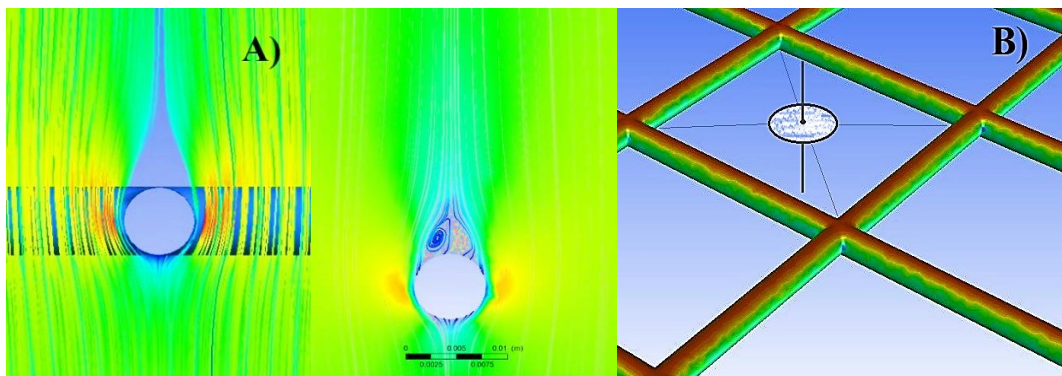


Figure 3: A) Streamlines and development of vortices around metal wires, B) Centre line for CFD measurements and stagnation pressure

Figure 4 shows the amount of pressure drop and velocity measured for different aperture sizes,  $\frac{d}{L}$ , during flow of  $N_2$  vapor through the metal screens. The measurements are done after the pressure shocks in either side of the metal screen are settled down and fully developed flow regime is reached. High tendency of both pressure differential and flow velocity variables to level off after certain aperture sizes results in the necessity of optimizing the porosity of wire woven mesh metals.

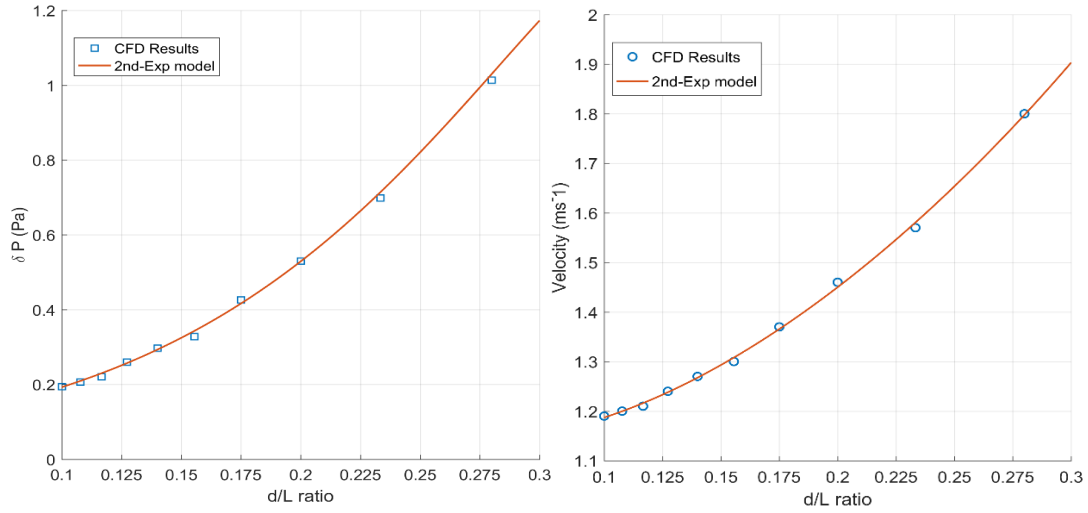


Figure 4: Pressure drops and velocity measurements for nitrogen vapor flow in ten aperture sizes.

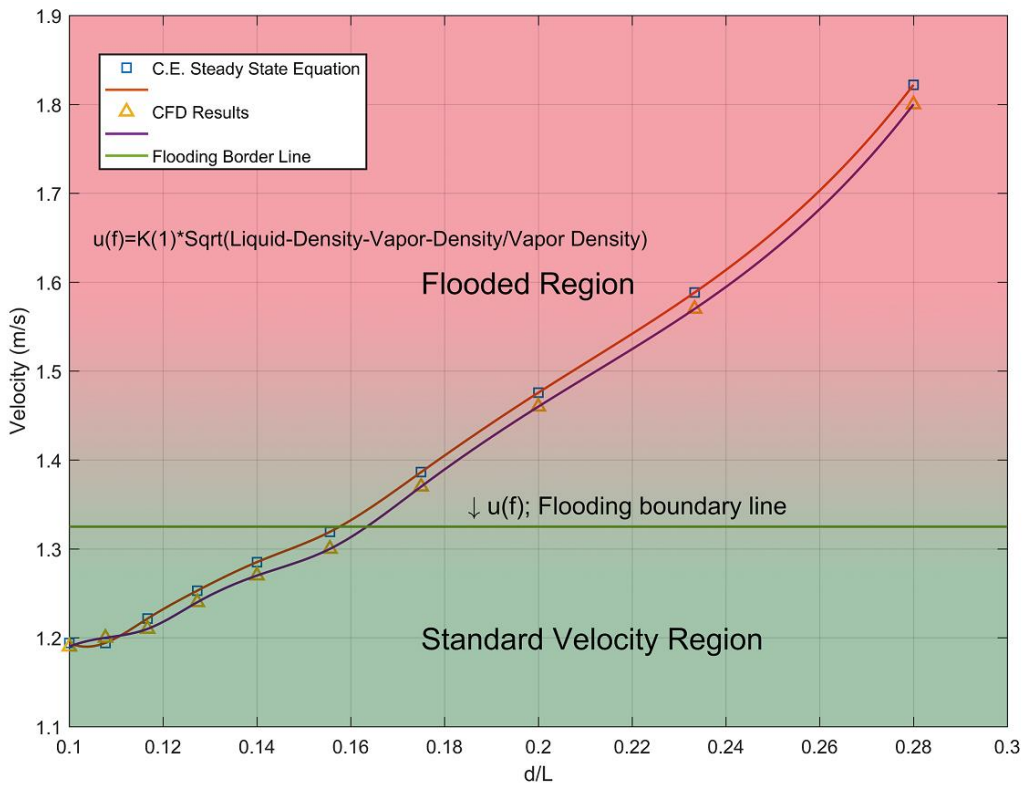


Figure 5: CFD results, vapor flooding point and validation in terms of porosity ratio,  $\frac{d}{L}$ .

In terms of velocity, the flooding point, that is based on 25% excessive value for design flow rate, is shown in figure 5. The graph consists of standard and flooded regions. This gives an inside into standard aperture size selection for metal meshes to avoid flooding condition in the packing voids. Towler & Sinnott also used vapor liquid flow factor and packed tower Y factor to locate the flooding and weeping point in generalized pressure drop correction chart [7].

All the FEA and CFD results are normalized and expressed in terms of porosity ratio,  $\frac{d}{L}$ , in figure 6. For FEA calculations, the desired conditions occur when normalized maximum deflection and stresses are minimal. Similarly, CFD analysis states that perturbed vapor design velocity and pressure drops should be minimized. The vertical line is a limit for flooding and weeping conditions. Using simplex method (graphical solutions), the optimized points can be detected by analyzing critical intersections of the 2<sup>nd</sup> degree exponential functions for each graph. These points are representative of the best porosity ratio,  $\frac{d}{L}$ , in which FEA and CFD requirements are addressed.

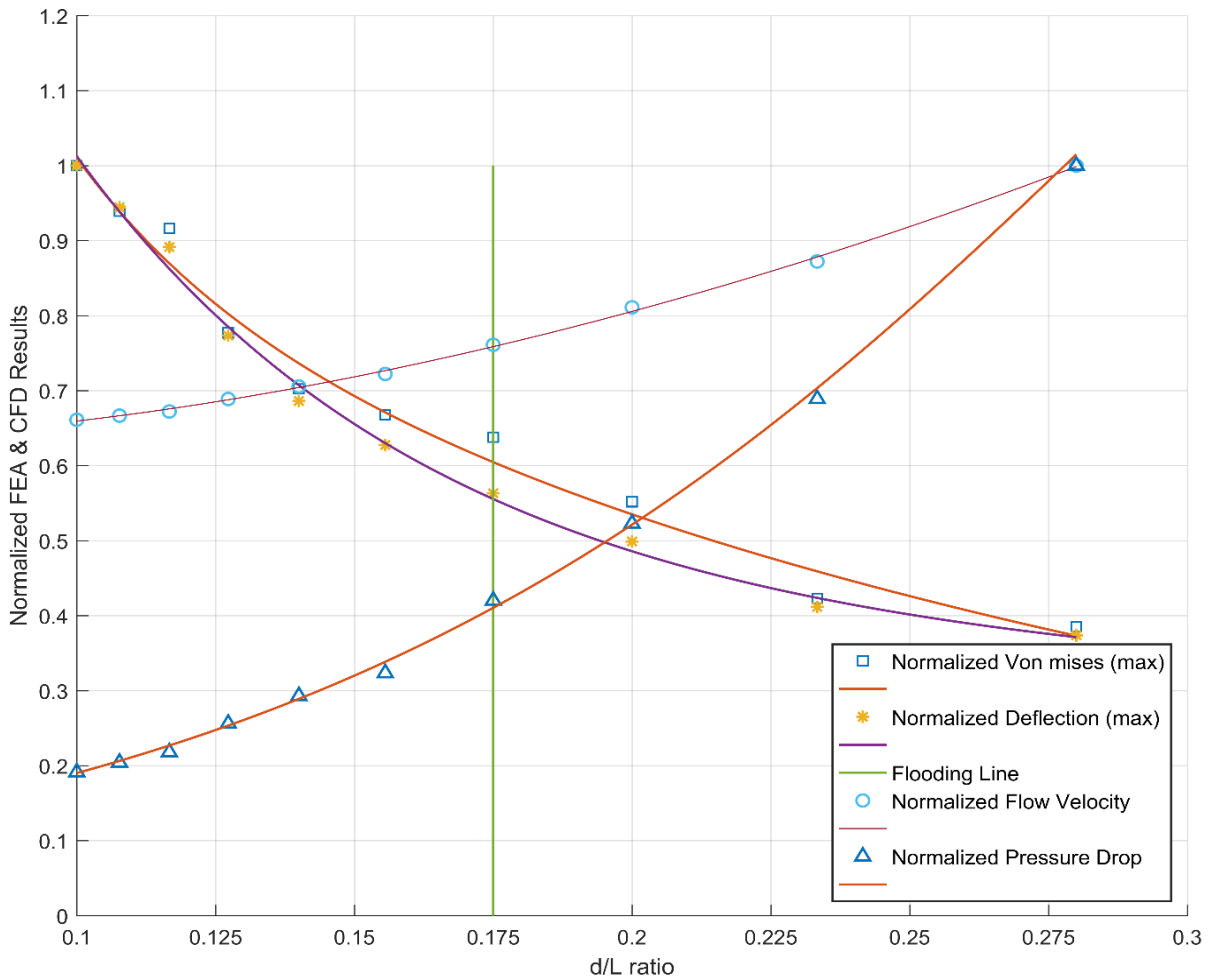


Figure 6: Combined normalized FEA and CFD results in terms of porosity ratio,  $\frac{d}{L}$

### 3.2 Validations

The pressure-drop results using Ansys (Fluent) are validated with the mathematical modellings produced by other authors. Sharifian, Wiegardt and Wakeland introduced their experimental equations to represent the pressure drop through metal wire woven meshes [8-10].

$$\Delta P = 0.5\rho U^2 \left( -0.491 + \frac{0.47}{p^{1.773}} - \frac{7.49}{Re^{0.661}} + \frac{6.475}{p^{2.244}Re^{0.661}} \right) \quad (1)$$

$$\Delta P = 0.5 \left( \frac{\rho U d}{\mu \beta} \right)^{-\frac{1}{3}} \left( 5.5 * \frac{1-\beta}{\beta^2} \right) \rho U^2 \quad (2)$$

$$\Delta P = 0.5 \left( \frac{\rho U d}{\mu} \right)^{-1/3} \left( 4.6 * \frac{1-\beta}{\beta^2} \right) \rho U^2 \quad (3)$$

where Re is the Reynolds number, p is the porosity ratio, d is the distance between neighboring metal wires, ρ is density, U is the free stream velocity, μ is the dynamic viscosity, and β is the ratio between aperture projected area with no blocking from filaments to total projected area;

$$\beta = \left( 1 - \frac{d}{L} \right)^2 \quad (4)$$

The results using the equations 1-3 are then plotted along with CFD results for pressure drop, in figure 7. Similarly, using the steady state flow assumption, the flow velocity is then validated by equation 5. The velocities are then plotted and compared to CFD results in figure 5. The comparison for both pressure-drops and flow velocities shows an acceptable accuracy.

$$U = \sqrt{0.64 K_1^2 * \frac{\rho_L - \rho_v}{\rho_v} - \frac{2(P_1 - P_2)}{\rho}} \quad (5)$$

where  $K_1$  is a flooding velocity coefficient for towers,  $\rho_L$  and  $\rho_v$  are liquid and vapor density, and  $P_1$  and  $P_2$  are fluid pressure before and after the metal mesh [11].

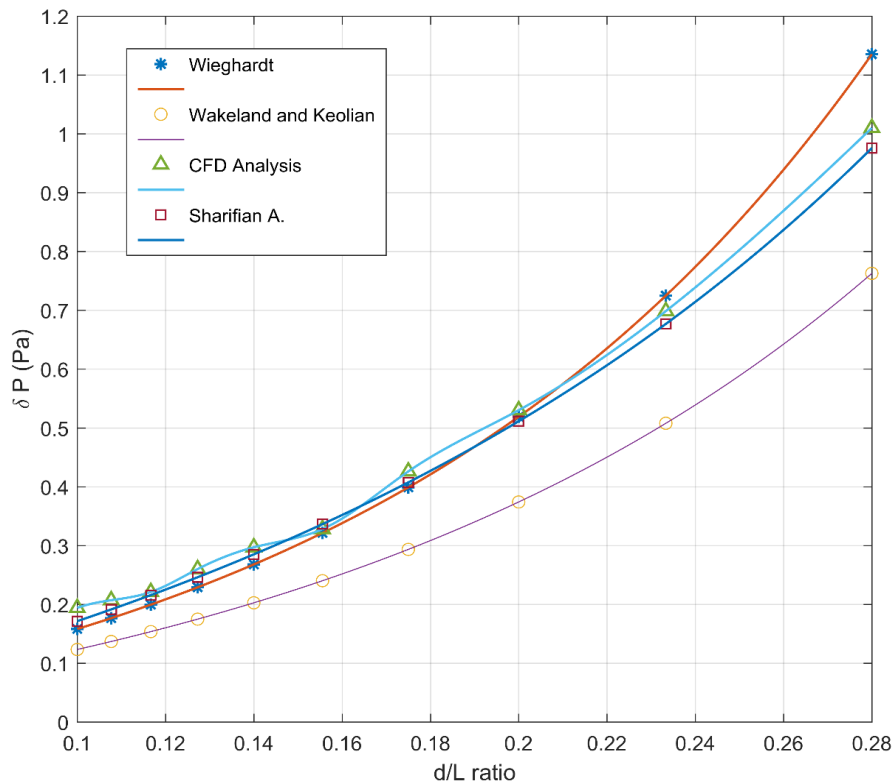


Figure 7: Validation of CFD analysis for Nitrogen pressure drops, in terms of porosity ratio,  $\frac{d}{L}$ .

#### 4 CONCLUSIONS

Effects of different aperture sizes on the mechanics behavior of fluid vapor, stresses and deflections in the metal mesh screens (WBC and Textile core representatives) investigated. Second order exponential function models used to simulate the plots with higher accuracy. The results indicate the behavior of both fluid characteristics and solid mechanics tend to be opposite each other. Thus, as the desired design condition is based on minimization of these values, the optimum design condition fell in the middle section of normalized graphs, and between the intersection of normalized fluid dynamics and solid mechanics graphs. By simplex optimization method (graphical solution), all these intersection points can be evaluated based on the significance of the different factors in each project.

Moreover, the combined and normalized diagrams can also give an optimized porosity ratio ranges,  $\frac{d}{L}$ , for design of the recommended WBC and textile core metal matrixes, when both fluid characteristics and structural integrity of any specific type of truss-like PCM is of importance. Meanwhile, same normalized and combined CFD-FEA diagrams can be generated for other types of truss-like PCMs, such as WBK and WBD. These diagrams that are expressed in terms of porosity ratios, can also be representative of other types of working fluids. Same pattern and behavior are predicted for different cases, with subtle changes in the intersections of FEA and CFD results.

#### ACKNOWLEDGEMENTS

The authors would like to thank University of Southern Queensland ([www.usq.edu.au](http://www.usq.edu.au)) for funding this research project. The authors would also like to thank Australian Institute of Advanced Studies ([www.aus-ias.edu.au](http://www.aus-ias.edu.au)) for providing access to the software packages and Mike Crawley ([mike@aus-ias.edu.au](mailto:mike@aus-ias.edu.au)) for enhancing plot visualizations to accomplish this research.

#### REFERENCES

- [1] K.J. Kang, *Wire-woven cellular metals: The present and future*, Progress in Material Science, Vol. 69, pp 213-307, 2015.
- [2] P. Zitha, J. Banhart and G. Verbist “Challenges and opportunities Eurofoam”. *MIT-Verlag Bremen*, pp 13-20, 2000.
- [3] M.G. Lee and K.J. Kang “Feasibility of a wire-woven metal for application as a sandwich panel”. *Journal of Mechanical Science*, Vol. 80, pp 81-92, 2014.
- [4] I. Sheldon, Z. Wang, T. Waung and A.Vakil “Simulation of flow through woven fabrics”. *Journal of Computers & Fluids*, Vol. 37, pp 1148-1156, 2008.
- [5] R. Hunt, Ed. Bausbacher “*Process Plant Layout & Piping Design*”. 1<sup>st</sup> edition, Prentice-Hall, 1993.
- [6] J.M. Coulson, J.F. Richardson “*Chemical Engineering*”. 4<sup>th</sup> edition, Vol. 6. pp 11-13, 2005.
- [7] G. Toller, R. Sinnott “*Chemical Engineering Design; principles, practice and economics of plant and process design*”. 2<sup>nd</sup> edition, Elsevier, 2013.
- [8] A. Sharifian, D.R. Buttsworth, Computational simulation of the wind-force on metal meshes, *Proceedings of 16th Australasian Fluid Mechanics Conference*, Gold Coast, December 2-7, 2007.
- [9] K.E.G. Wieghardt, On the resistance of screens, *The Aeronautical Quarterly*, Vol. 4, pp. 186-97, 1953.
- [10] R.S. Wakeland, R.M. Keolian, Measurements of resistance of individual square-mesh screens to oscillating flow at low and intermediate Reynolds numbers, *Journal of Fluids Engineering*, Vol. 125, pp. 851-62, 2003.
- [11] J.M. Coulson, J. Richardson, “*Chemical Engineering Design*”, 3<sup>rd</sup> edition, Vol. 6. pp 567, 1994.